DOI: 10.1534/genetics.107.073890

A Genetic Mosaic Analysis With a Repressible Cell Marker Screen to Identify Genes Involved in Tracheal Cell Migration During Drosophila Air Sac Morphogenesis

Hélène Chanut-Delalande,*,[1] Alain C. Jung,*,[1] Li Lin,*,[1,2] Magdalena M. Baer,† Andreas Bilstein,† Clemens Cabernard,*,[3] Maria Leptin† and Markus Affolter*,[4]

**Biozentrum der Universität Basel, Abt. Zellbiologie, CH-4056 Basel, Switzerland and* †*Institut für Genetik, Universität zu Köln, D-50674 Köln, Germany*

Manuscript received April 2, 2007
Accepted for publication June 1, 2007

ABSTRACT

Branching morphogenesis of the Drosophila tracheal system relies on the fibroblast growth factor receptor (FGFR) signaling pathway. The Drosophila FGF ligand Branchless (Bnl) and the FGFR Breathless (Btl/FGFR) are required for cell migration during the establishment of the interconnected network of tracheal tubes. However, due to an important maternal contribution of members of the FGFR pathway in the oocyte, a thorough genetic dissection of the role of components of the FGFR signaling cascade in tracheal cell migration is impossible in the embryo. To bypass this shortcoming, we studied tracheal cell migration in the dorsal air sac primordium, a structure that forms during late larval development. Using a mosaic analysis with a repressible cell marker (MARCM) clone approach in mosaic animals, combined with an ethyl methanesulfonate (EMS)-mutagenesis screen of the left arm of the second chromosome, we identified novel genes implicated in cell migration. We screened 1123 mutagenized lines and identified 47 lines displaying tracheal cell migration defects in the air sac primordium. Using complementation analyses based on lethality, mutations in 20 of these lines were genetically mapped to specific genomic areas. Three of the mutants were mapped to either the *Mhc* or the *stam* complementation groups. Further experiments confirmed that these genes are required for cell migration in the tracheal air sac primordium.

REGULATION of gas and fluid exchanges at the level of barrier epithelia is a key feature common to all organisms of the animal kingdom. To achieve this function, epithelia often acquire a tubular architecture where functional units occur repetitively, form in many cases an interconnected network, and create a large interface of interaction with their environment. This organization is achieved during embryogenesis via a process called branching morphogenesis, which relies on distinct cellular behavior often including cell division, cell migration, cell rearrangements, cell shape changes, and cell death (Hogan and Kolodziej 2002; Affolter *et al.* 2003; Lubarsky and Krasnow 2003). Growth factors, including fibroblast growth factor (FGF) molecules, are known to be crucial for the regulation of these processes (Warburton *et al.* 2000; Ghabrial *et al.* 2003).

In *Drosophila melanogaster*, Breathless/fibroblast growth factor receptor (Btl/FGFR) is implicated in the Branchless/FGF (Bnl/FGF)-dependent migration of tracheal cells during the development of the embryonic tracheal system (Klambt *et al.* 1992; Sutherland *et al.* 1996; Affolter *et al.* 2003; Ghabrial *et al.* 2003; Uv *et al.* 2003). Btl/FGFR is expressed in migrating tracheal cells, whereas the Bnl/FGF ligand is expressed in single or groups of ectodermal and mesodermal cells, in a highly dynamic pattern that prefigures tracheal branch outgrowth. In the absence of either the receptor or the ligand, tracheal cells do not migrate. Additional factors including the cytoplasmic adaptor Downstream-of-FGFR (Dof) and the FGFR coreceptors Sulfateless (Slf) and Sugarless (Sgl) have been shown to be required for FGFR signaling (Michelson *et al.* 1998; Vincent *et al.* 1998; Imam *et al.* 1999; Lin *et al.* 1999; Pellegrini 2001). However, the important maternal contribution of proteins of the Ras/MAP kinase pathway to the egg makes it difficult to link the function of this signaling cassette to FGFR-dependent cell migration, as the homozygous mutant offspring of heterozygous parents show no phenotype (Affolter and Weijer 2005). In addition, eggs deriving from homozygous female germ-line clone-bearing mutations affecting genes of the Ras/MAP

[1]These authors contributed equally to this work.

[2]*Present address:* Department of Biochemistry and Biophysics, University of California, San Francisco, CA 94143.

[3]*Present address:* Institute of Molecular Biology, University of Oregon, Eugene, OR 97403.

[4]*Corresponding author:* Biozentrum der Universität Basel, Klingelbergstrasse 70, CH-4056 Basel, Switzerland. E-mail: markus.affolter@unibas.ch

kinase pathway display extremely severe developmental defects, hindering any detailed analysis in the tracheal system. This shortcoming can be circumvented to a large extent by analyzing clones of mutant cells in mosaic Drosophila larvae, where much of the maternal contribution has been consumed. Interestingly, during late larval development, the tracheal system is extensively remodeled to give rise to the adult respiratory organs (Whitten 1980; Manning and Krasnow 1993). During this period, a structure referred to as the dorsal air sac primordium buds from a tracheal branch called the transverse connective, in the second thoracic segment, and undergoes a morphogenetic process that relies both on cell division and on cell migration (Sato and Kornberg 2002; Guha and Kornberg 2005). The mosaic analysis with a repressible cell marker (MARCM) clone technique (Lee and Luo 1999, 2001) has been adapted to genetically dissect tracheal cell migration and proliferation in the developing dorsal air sac primordium (Cabernard and Affolter 2005). It was shown that while cell proliferation and survival in the primordium require the epidermal growth factor receptor (EGFR) signaling pathway, FGFR signaling is strictly required for tracheal cell migration at the tip of the primordium (Sato and Kornberg 2002; Cabernard and Affolter 2005). The effects of both EGFR and FGFR require the Ras/MAP kinase cassette. Interestingly, the ETS transcription factor Pointed (Brunner *et al.* 1994; O'Neill *et al.* 1994) is required exclusively for FGF-dependent cell migration, but dispensable for EGF-regulated cell division/survival (Cabernard and Affolter 2005). Although these studies provide evidences that the Ras/MAP kinase pathway is involved in tracheoblast migration, additional factors involved in interpreting either the FGF or the EGF signal remain to be identified.

To gain further insight into the regulation of FGF-dependent tracheal cell migration, we took advantage of the MARCM clone technique and carried out a large-scale screen of a collection of fly lines carrying randomly induced mutations. In this article, we describe a screening approach that allowed us to successfully isolate mutant fly strains displaying tracheal cell migration defects during the morphogenesis of the dorsal air sac primordium. We also present the identification of two complementation groups required for cell migration during air sac morphogenesis.

MATERIALS AND METHODS

Drosophila stocks: *D. melanogaster* lines were raised at 25° using standard conditions. Ethyl methanesulfonate (EMS) mutant lines were generated according to standard mutagenesis procedures (see accompanying article by Baer *et al.* 2007, this issue). Isogenic *FRT40A* males were fed on 30 mm EMS to generate random mutations in the genome. The following MARCM strain (Cabernard and Affolter 2005) was used during the screen: *70hsFLP/70hsFLP; tubGal80, FRT40A/CyO*; *btlenhancer-mRFP1moe, btlGal4-UAS-CD8-GFP/TM6C*. Deficiency lines generated by Exelixis (Parks *et al.* 2004) were used for complementation tests. The following mutant lines were used to map lethal hits and/or to recover MARCM mutant clones: *btlH82delta3* (Reichman-Fried *et al.* 1994), glu^{k08819}, Mhc^{1}, Mhc^{3}, Mhc^{4} (Mogami *et al.* 1986), and Mhc^{3}, *FRT40A* (kindly provided by P. Rorth) (Borghese *et al.* 2006). The Mhc^{1} mutant allele was recombined with *FRT40A* using standard genetic methods.

Generation of MARCM clones in the developing air sac primordium: MARCM clones were generated following the procedure described previously in Cabernard and Affolter (2005). MARCM virgin females were crossed *en masse* to the mutant *FRT40A* lines of interest. Embryos of the progeny were submitted to a heat shock 4–6 hr after egg laying for 1 hr at 38° in a circulating water bath and kept at 25° until larvae reached third instar. Third instar larvae bearing GFP-positive clones were collected using a Leica MZFLIII GFP stereomicroscope. Larval wing discs were dissected in PBS and mounted in Schneider Cell Medium (GIBCO, Grand Island, NY). Pictures of air sac primordia were taken using a Leica TCS SP2 confocal system with the Leica Confocal Software and deconvoluted with Huygens Essential (Version 2.3.0) and subsequently processed with the Imaris 4.0.4 software (Bitplane).

Mapping of lethal mutations: Lethal mutations induced on the left arm of the second chromosome were genetically mapped by screening for noncomplementation of lethality, using deficiencies generated by Exelixis, which uncover 80% of the left arm of the second chromosome (Thibault *et al.* 2004). In a further candidate gene approach, known lethal mutations affecting genes located in the genomic regions determined by deficiency mapping were tested for lethality in *trans* to mutant candidate lines. Other mutant lines were obtained from the Bloomington Stock Center.

Rescue constructs: To generate a *UAS-stam* rescue construct, a full-length s*tam* cDNA (LD02639) was subcloned into the *pUAST* vector. Transgenic flies were generated according to standard transformation protocols. Only insertions in the third chromosome were kept for the rescue experiments performed in combination with MARCM analysis.

Sequencing experiments: Identification of the affected gene for the *2L2896* and *2L3297* lines was achieved by DNA sequencing. The *2L2896* and *2L3297* lines were balanced over a *CyO-YFP* balancer chromosome. YFP-negative homozygous mutant embryos were sorted using a Leica MZFLIII GFP stereomicroscope. Genomic DNA from these embryos was extracted and used as a template for PCR amplification of the Stam, *Ial*, and *Dnz1* coding regions. Primers were designed along these DNA regions to sequence the entire open reading frames. The primer pairs that yielded the point mutations for the *2L2896* line have the following sequences: 5′-GGTCTACG CAGGAGGAAGTACACC-3′ and 5′-CTCAATCGGGGGATC GGG-3′ for the C^{16}-to-T substitution and 5′-CGGGTGGAT TCCCACCGG-3′ for the G^{1513}-to-A substitution. The following primers allowed the identification of the mutations in the *2L3297* lines: 5′-CCGAGCTGGAACGCGTCG-3′ and 5′-GTGG CACCTGCCCCTGCGG-3′ for the T^{1283}-to-C substitution and 5′-CGGGTGGATTCCCACCGG-3′ and 5′-CCCTGTGGTGGC GGTGCC-3′ for the T^{1583}-to-C substitution.

RESULTS

Screen procedure overview: To identify genes involved in FGF-dependent migration of tracheal cells

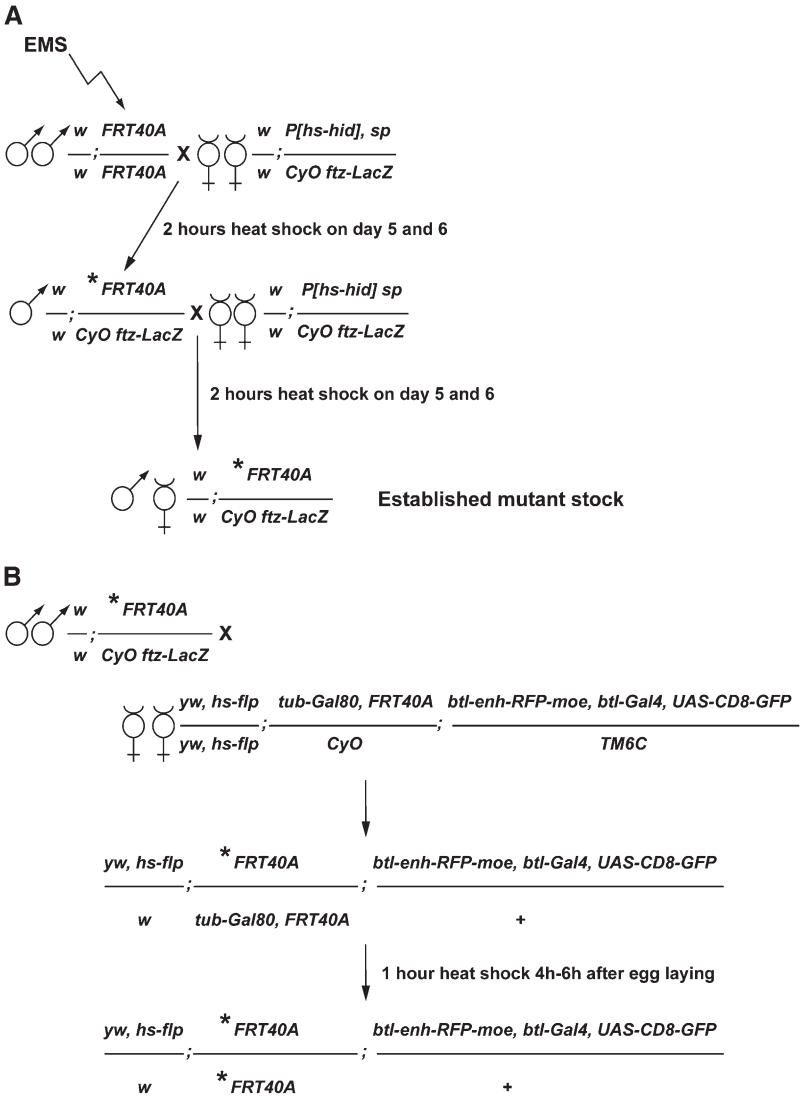

Figure 1.—Mutagenesis and crossing scheme to generate MARCM clones of cells homozygous for mutations on chromosome 2L. (A) Scheme for the establishment of Drosophila stocks carrying mutations on the second chromosome. Ethyl methanesulfonate (EMS)-induced mutations were randomly generated in the genome of males bearing a *FRT40A* chromosome. EMS-treated males were subsequently crossed to females carrying an *hs-hid* construct and a balancer chromosome. The asterisk represents the induced mutation. Balanced mutant stocks were established in two generations. A heat-shock regime applied to the progeny of the F_0 and F_1 generation induced the expression of the *hs-hid* construct and the death of animals due to ectopic apoptosis. Therefore, establishment of the heterozygous mutant stocks did not require virgin female collection. (B) Crossing scheme to induce MARCM clones in the Drosophila larval tracheal system. F_2 heterozygous mutant males were crossed to so-called MARCM females carrying a *heat-shock-flipase* (*hs-flp*) source, a *FRT40A* chromosome recombined to a *tubulin-Gal80* (*tub-Gal80*) construct, and a third chromosome bearing the *breathless-Gal4* (*btl-Gal4*), *UAS-CD8-green fluorescent protein* (*UAS-CD8-GFP*), and *breathless enhancer-red fluorescent protein-moesin* (*btl-enh-RFP-moe*) constructs. Heat-shock treatment of generation F_3 induced the Flp-driven recombination at FRT sequences, which segregate the *tub-Gal80* construct away from the induced mutation. Therefore, the *btl-Gal4*-dependent expression of CD8-GFP was possible only in clones of cells homozygous for the induced mutation (see also Figure 3A).

during morphogenesis of the dorsal air sac primordium in Drosophila, we carried out a large-scale mosaic MARCM clone screen (Lee and Luo 1999, 2001) for fly lines displaying cell migration defects. We designed a F_3 mutagenesis scheme to establish mutant fly stocks carrying random EMS-induced mutations. Since our analysis was focused on genes located on the left arm of the second chromosome, we used a *FRT40A* chromosome in the EMS-treated stock (Figure 1A and accompanying article by Baer *et al.* 2007).

To induce MARCM mutant clones, ~10 males of each of these putative heterozygous mutant lines were crossed *en masse* to ~30 so-called *FRT40A* MARCM females; these females carry a *heat-shock-flipase* (*hs-flp*) source, a *FRT40A* chromosome recombined to a *tubulin-Gal80* (*tub-Gal80*) construct, and a third chromosome bearing a *breathless-Gal4* (*btl-Gal4*), a *UAS-CD8-green fluorescent protein* (*UAS-CD8-GFP*), and a *breathless enhancer-red fluorescent protein-moesin* (*btl-enh-RFP-moe*) construct (Cabernard and Affolter 2005) (Figure 1B). Using this genetic setup, mutant clones can be induced via FLP-mediated recombination at FRT40A sites in early embryonic stages, and visualized as GFP-positive groups of cells following the loss of Gal80. The Gal80-independent action of the *btl* enhancer enables the visualization of the entire tracheal system by expression of the *RFP-moe* fusion construct (Figure 2, C, E, and F). The dorsal air sac primordium buds from a tracheal branch called the transverse connective (TC) in the second thoracic segment (Figure 2A) and grows on the underlying wing imaginal disc during the third larval instar period (Sato and Kornberg 2002; Guha and Kornberg 2005) (Figure 2B). FLP-driven recombination was induced in the early embryo according to the procedure described (Cabernard and Affolter 2005). Embryos were subsequently allowed to develop and third instar larvae displaying GFP-labeled patches of cells in the tracheal system were collected (Figure 2D). Wing discs were dissected and air sac primordia bearing MARCM clones were analyzed using laser confocal

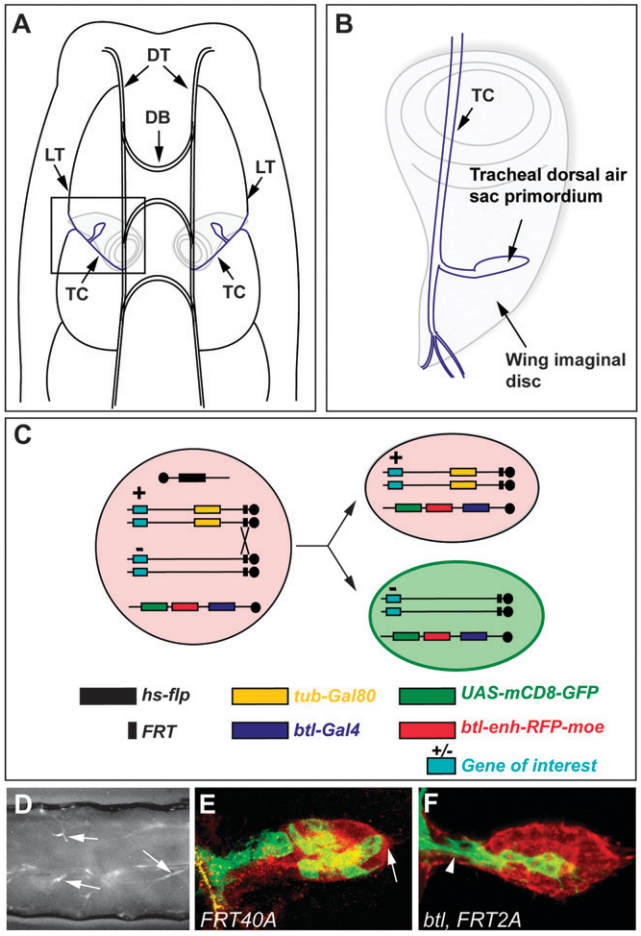

FIGURE 2.—Localization of the dorsal air sac primordium in a Drosophila larva and generation and visualization of MARCM clones in the air sac primordium. (A) Schematic representation of the dorsal view of a Drosophila larva. The dorsal air sac primordium (blue) buds from a tracheal branch called the transverse connective (TC) and grows on the underlying wing imaginal disc (gray). DT, dorsal trunk; DB, dorsal branch; LT, lateral trunk; TC, transverse connective. (B) Schematic representation of the localization of a dorsal air sac primordium on the wing imaginal disc: magnification of the inset shown in A. (C) Schematic representation of the induction of MARCM clones. In all cells of animals heterozygous for the mutation of interest (+/−), the expression of the Gal80 repressor, which is under the control of a *tubulin* promoter, inhibits the Gal4-dependent expression of CD8-GFP. The expression of RFP-moesin is driven in all tracheal cells by the *btl* enhancer (red background). Upon heat-shock treatment of heterozygous animals, Flp expression is induced and drives the site-directed recombination at FRT sites, which ultimately leads, after mitosis, to the segregation of Gal80 and Gal4. The expression of CD8-GFP (green background) is therefore induced in cells homozygous for the mutation of interest (−/−). (D) GFP stereomicroscope view of a Drosophila larva of the F_3 generation (see Figure 1B), after heat-shock treatment. Arrows indicate GFP-positive MARCM clones scattered in the tracheal system. Anterior is to the left, dorsal is up. (E and F) Confocal micrographs of a Drosophila third instar larval dorsal air sac primordium. All tracheal cells are labeled in red (RFP-moesin). Cells belonging to the MARCM clones are labeled in green (CD8-GFP). Clones are homozygous for a *FRT40A* (E) or *btl, FRT42A* chromosome (F). Arrows indicate the distal tip of the air sac primordium. Arrowheads indicate the proximal region of the air sac primordium.

microscopy in live tissues (Figure 2, E and F), without any fixation or staining requirement.

It has previously been reported that MARCM clones of wild-type cells contribute to the growing tip of the air sac primordium (arrow in Figure 2E) in ~70% of the cases (CABERNARD and AFFOLTER 2005). It was also shown that the FGFR signaling pathway is crucial for tracheal cell migration, as MARCM clones mutant for the Drosophila *btl/FGFR* or for certain downstream effectors of the FGFR signaling pathway remain in the proximal region of the air sac primordium (arrowhead in Figure 2F) and never colonize the migrating tip of the primordium (CABERNARD *et al.* 2004). In an attempt to isolate genes involved in tracheal cell migration, mutant lines displaying a migration defect with <40% of the MARCM clones present at the air sac distal tip were kept for further analysis. Putative mutant lines were systematically retested a second and eventually a third time.

Screen result overview: A total of 1123 lines were screened. Statistical distribution of the different phenotypes with respect to the presence/absence and localization of MARCM clones is summarized in Table 1. In 11% ($N = 122$) of the lines, we did not recover any individuals displaying MARCM clones in the larval tracheal system. In 8% ($N = 90$) of the lines, clones were observed in the tracheal system, but not recovered in the air sac primordium. In 77% ($N = 864$) of the lines tested, MARCM clones showed wild-type behavior, as GFP-labeled clones colonized the air sac primordium distal tip according to wild-type frequencies.

In the remaining lines (4%; $N = 47$), a consistent phenotype was observed with respect to two criteria: the position of MARCM clones within the air sac primordium and the size distribution of the MARCM clones. Indeed, it has been shown previously that MARCM clones mutant for components of the Ras/MAPK pathway display both a migration phenotype and a proliferation defect, since mutant clone sizes are rather small when compared to marked wild-type clones (CABERNARD and AFFOLTER 2005). In contrast, MARCM clones homozygous for *btl/FGFR* grow normally, but never populate the air sac primordium distal tip (CABERNARD and AFFOLTER 2005). Taking these two aspects into consideration, we assigned the 47 lines displaying a migration phenotype to two distinct classes (Table 1): mutant lines displaying a strict migration phenotype (showing wild-type-like clone sizes) were assigned to class I, whereas lines showing both a migration phenotype and a reduced clone size distribution were assigned to class II.

Class I mutants: The class I category consisted of 38 fly lines (compare Figure 3, B–D, to Figure 3A). Thirty-four class I mutant lines were homozygous lethal, and 4 lines were homozygous viable (Tables 1 and 2). Two of the 34 homozygous lethal mutant class I lines (*2L3267* and *2L2870*) displayed a phenotype similar to the complete

TABLE 1

Overview of the screen

Tested mutant lines	1123
Lines with larvae displaying no MARCM clones	122 (11%)
Lines with air sacs displaying no MARCM clones	90 (8%)
Lines showing no tracheal cell migration and proliferation phenotype	864 (77%)
Lines showing a tracheal cell migration phenotype (class I)	38
Class I lethal lines	34
Class I not lethal lines	4
Lines showing a tracheal cell proliferation phenotype (class II)	9
Class II lethal lines	8
Class II not lethal lines	1

A total of 1123 lines were tested. Numbers refer to the amount of lines for which F_3 third instar larvae displayed a given phenotype after heat-shock treatment and induction of MARCM clones. Percentage values shown in parentheses refer to the total number of strains that were tested. Lines displaying a tracheal cell migration phenotype were classified in two categories: class I (strict migration phenotype) and class II (migration and proliferation phenotype). In both categories, lethal and viable alleles were recovered.

loss of FGF signaling; *i.e.*, no clones were observed at the distal tip of the air sac primordium (Table 2 and Figure 3D). In the other class I mutants, the statistical distribution of MARCM clones at the distal tip ranked from 3.3 to 38.1% (Table 2).

Class II mutants: Class II contains nine mutant lines, MARCM clones of which displayed both a migration and a proliferation phenotype (compare Figure 3, E and F, to Figure 3A). Eight class II mutants were homozygous lethal, and one was homozygous viable (Tables 1 and 3).

As our aim was to identify genes implicated in FGF-driven tracheal cell migration, we started our analysis with class I mutants, which show a strict migration phenotype. Since the FGFR signaling pathway is crucial for numerous steps throughout development, mutations affecting factors playing important roles in this pathway are likely to be homozygous lethal. Thus, we have chosen to focus our analysis on those 34 class I mutants that were homozygous lethal. Our strategy to identify genes involved in distal tip cell migration during dorsal air sac development was the following. First, we identified the lethal hit in the mutant line. Second, we investigated whether the gene responsible for lethality was indeed involved in distal tip migration, either by performing rescue experiments in MARCM clones or via the identification of additional mutations in the same gene and testing whether these mutations caused the same MARCM mutant phenotype (Tables 1 and 2).

Mapping of class I mutants and complementation analysis: Lethal hits in candidate lines were mapped using complementation analysis. We took advantage of the Exelixis targeted deficiency kit, as each deficiency uncovers only ~25 genes (Parks *et al.* 2004). Exelixis deficiencies cover ~80% of transcription units of chromosomal arm 2L described by the FlyBase Consortium. All the EMS mutant lines were crossed to homozygous lethal Exelixis deficiency lines and the progeny of these crosses was scored for the absence of viable *trans*-heterozygotes. This approach allowed us to map

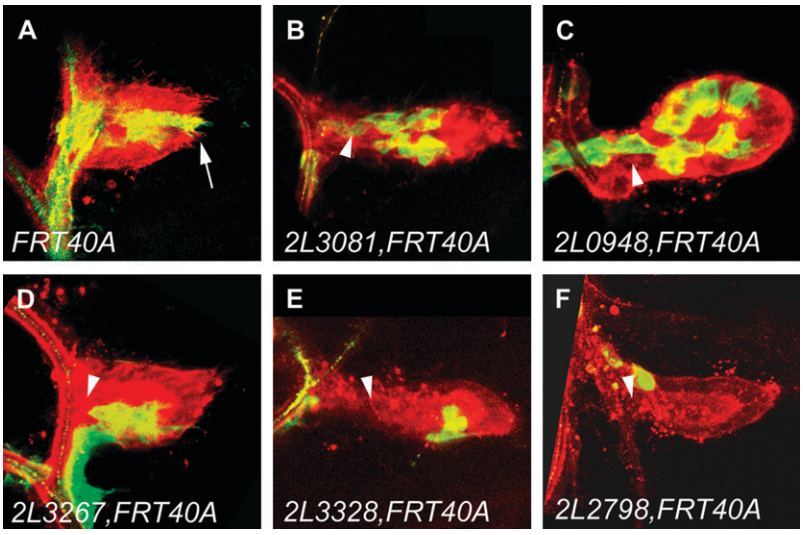

Figure 3.—Migration defects of various mutants isolated during the screen. Confocal micrographs of the dorsal air sac primordium of a Drosophila third instar larva are shown. All tracheal cells are labeled in red (RFP-moesin) and MARCM clones are labeled in green (CD8-GFP). The *FRT40A* chromosome (A) was used as a wild-type control. Isolated mutants were classified in two categories (see also Table 1): class I mutants, characterized by a strict migration phenotype and displaying clones of normal size, such as observed in the lines *2L3081, FRT40A* (B), *2L0948, FRT40A* (C), and *2L3267, FRT40A* (D), and class II mutants, showing a migration defect and additionally a reduced size of MARCM clones, such as observed in lines *2L3328, FRT40A* (E) and *2L2798, FRT40A* (F). Arrows indicate the distal tip of the air sac primordium. Arrowheads indicate the proximal region of the air sac primordium.

TABLE 2

Overview of the phenotype and mapping of the isolated class I mutant lines

	Clones at the distal tip	Clones at the proximal region	Analyzed clones	% at the distal tip	Lethal line	Mapping to	Does not complement to	Identified gene
2L 3267	0	26	26	0.0	Yes	Df(2L)exel6039, 8036		
2L 2870	0	39	39	0.0	Yes			
2L 2677	1	29	30	3.3	Yes			
2L 2436	1	15	16	6.3	Yes	Df(2L)exel8012, 7021		
2L 3186	1	13	14	7.1	Yes	Df(2L)exel7038		
2L 3189	1	12	13	7.7	Yes			
2L 3081	4	31	35	11.4	Yes	Df(2L)exel8038		
2L 2881	2	14	16	12.5	Yes	Df(2L)exel6027, 7067	*mhc1*	*mhc*
2L 3298	1	6	7	14.3	Yes	Df(2L)exel7034		
2L 2475	1	6	7	14.3	Yes	Df(2L)exel6042	*2L1665*	
2L 2653	2	11	13	15.4	Yes	Df(2L)exel6047, 7055		
2L 1683	2	11	13	15.4	Yes	Df(2L)exel7038		
2L 3297	4	21	25	16.0	Yes	Df(2L)exel8026, 7049	*2L2896*	*stam*
2L 2896	5	24	29	17.2	Yes	Df(2L)exel7038, 8026, 7049	*2L3297*	*stam*
2L 2828	6	26	32	18.8	Yes			
2L 2985	4	15	19	21.1	Yes			
2L 3073	3	10	13	23.1	Yes			
2L 2845	10	32	42	23.8	Yes			
2L 2853	8	25	33	24.2	Yes			
2L 2718	2	5	7	28.6	Yes			
2L 2775	7	17	24	29.2	Yes	Df(2L)exel6028		
2L 1710	4	9	13	30.8	Yes			
2L 1685	7	15	22	31.8	Yes	Df(2L)exel8003		
2L 948	9	18	27	33.3	Yes			
2L 2921	6	12	18	33.3	Yes			
2L 1561	3	6	9	33.3	Yes	Df(2L)exel6042		
2L 1540	12	22	34	35.3	Yes	Df(2L)exel6044		
2L 1809	10	18	28	35.7	Yes			
2L 2938	9	16	25	36.0	Yes	Df(2L)exel6277		
2L 1665	9	16	25	36.0	Yes	Df(2L)exel6042	*2L2475*	
2L 3179	8	14	22	36.4	Yes	Df(2L)exel7022		
2L 2615	8	14	22	36.4	Yes	Df(2L)exel6031		
2L 3011	13	22	35	37.1	Yes	Df(2L)exel6042, 8040		
2L 1794	8	13	21	38.1	Yes			
2L 2468	1	7	8	12.5	No			
2L 2366	1	7	8	12.5	No			
2L 883	4	12	16	25.0	No			
2L 3064	7	15	22	31.8	No			

Lines displaying a strict tracheal cell migration phenotype, characterized by the observation of <40% of MARCM clones reaching the distal tip of the air sac primordium (see also Figure 3, B–D), were retained for further analysis (class I mutants). We recovered 38 strains meeting this criterion (see also Table 1). For each line, numbers refer to the amount of MARCM clones observed at the distal tip of the air sac primordium (column 2) and in the proximal region (column 3), to the total number of observed clones (column 4), and to the percentage of MARCM clones localized at the air sac primordium distal tip (column 5; Figure 3). We recovered 34 homozygous lethal lines and 4 homozygous viable lines. Exelixis deficiencies, other independent class I mutants or previously characterized alleles, and names of mutants belonging to the same complementation group as other class I mutants we isolated are indicated in columns 7, 8, and 9, respectively.

lethal hits in 20 mutant strains (Table 2). On the basis of these lethality tests, we found that 18 lines carried at least one lethal hit (no complementation between the lethal hit and either one deficiency or a group of overlapping deficiencies) and that 2 lines carried at least two lethal hits (no complementation between the lethal hit and two nonoverlapping deficiencies) on the left arm of the second chromosome.

Mutant lines mapping to the same genomic area were crossed *inter se* to determine whether they belonged to the same complementation group. Using this procedure, we found that *2L1665* and *2L2475*, both carrying a lethal hit mapping to *Df(2L)exel6042*, as well as *2L2896* and *2L3297*, carrying a lethal hit mapping to *Df (2L)exel7049* and *Df(2L)exel8026*, did not complement each other's lethality (Table 2), suggesting that these

TABLE 3

Overview of the phenotype of the isolated class II mutant lines

	Clones at the distal tip	Clones at the proximal region	Analyzed clones	% at the distal tip	Lethal line
2L 3194	0	7	7	0.0	Yes
2L 1748	0	3	3	0.0	Yes
2L 1682	0	5	5	0.0	Yes
2L 2983	0	1	1	0.0	Yes
2L 2834	0	3	3	0.0	Yes
2L 2798	0	7	7	0.0	Yes
2L 2686	3	23	26	11.5	Yes
2L 3328	3	21	24	12.5	Yes
2L 1738	4	15	19	21.1	No

Class II mutant lines displayed migration phenotypes meeting our screening criteria (<40% of MARCM clones reaching the air sac primordium distal tip). However, class II mutant lines also displayed MARCM clones of reduced size (see also Figure 3, E and F). We recovered nine strains meeting this criterion (see also Table 1). For each line, numbers refer to the amount of MARCM clones observed at the distal tip of the air sac primordium (column 2) and in the proximal region (column 3), to the total number of observed clones (column 4), and to the percentage of MARCM clones localized at the distal tip of the air sac primordium (column 5; Figure 3, E and F). We recovered eight homozygous lethal lines and one homozygous viable line.

mutations represent two independent alleles of the same gene.

To identify the affected loci in the 20 mapped mutant lines, we used available lethal mutations (previously isolated mutations or transposon insertions) in the region uncovered by the corresponding Exelixis deficiencies and tested whether these mutations complemented the lethality of the corresponding EMS-induced mutants. Alternatively, when no lethal mutation was available in the region of interest, a sequencing approach was used. These approaches led to the identification of two complementation groups responsible for lethality (see below).

Gene identification: *Mutant line 2L2881:* In *2L2881*, only 12.5% of the homozygous mutant MARCM clones were capable of reaching the distal tip of the air sac primordium (Table 2 and Figure 4, A and D).

Genetic mapping showed that the lethal mutation present in *2L2881* did not complement two overlapping Exelixis deficiencies, *Df(2L)Exel6027* and *Df(2L)Exel7067* (Table 2). This narrowed the region of interest down to 12 genes, including *gluon* (*glu*) and *Myosin heavy chain* (*Mhc*), two essential genes. Lethal alleles of *glu* (glu^{k08819}) and of *Mhc* [Mhc^{1}, Mhc^{3}, and Mhc^{4} (Mogami *et al.* 1986)] were then tested by complementation analysis; we found that the Mhc^{1}, Mhc^{3}, and Mhc^{4} alleles did not complement the lethality observed in *2L2881*, whereas glu^{k08819} did. These results suggested that *2L2881* carried a lethal hit in the *Mhc* gene.

We next tested whether mutations in *Mhc* displayed a phenotype similar to *2L2881* by analyzing the behavior of MARCM clones homozygous for the amorphic Mhc^{1} or the hypomorphic Mhc^{3} allele in the air sac primordium. To do so, we recombined the Mhc^{1} allele onto the *FRT40A* chromosome and used a previously described Mhc^{3}, *FTR40A* recombinant allele (Borghese *et al.* 2006), respectively. Although many air sac primordia were screened, only one tiny MARCM Mhc^{1}mutant

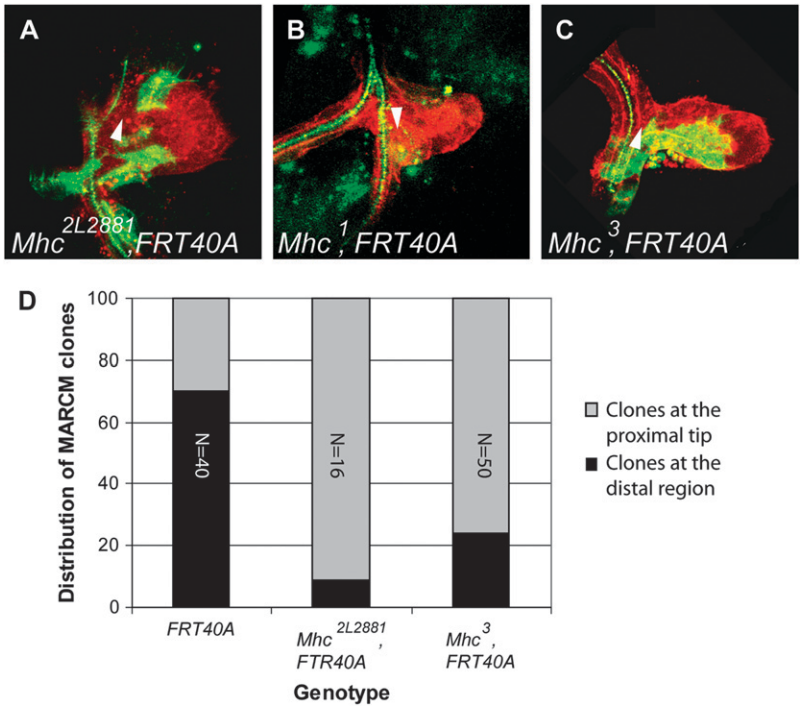

Figure 4.—Homozygous *Mhc* mutant MARCM clones display a migration phenotype. (A–C) Confocal micrographs of a Drosophila third instar larval dorsal air sac primordium. All tracheal cells are labeled in red (RFP-moesin). Cells belonging to the MARCM clones are labeled in green (CD8-GFP). MARCM clones were induced in individuals heterozygous for Mhc^{2L2881} (A), Mhc^{1} (B), and Mhc^{3} (C). Arrowheads indicate the proximal region of the air sac primordium. (D) Graphical representation of the statistical distribution of MARCM clones in the dorsal air sac primordium (gray, localization at the proximal region; black, localization at the distal growing tip). The *FRT40A* chromosome was used as a wild-type control. Wild-type clones colonize the distal growing air sac tip in 70% of the cases. This proportion is dramatically reduced in the Mhc^{2L2881} and Mhc^{3} mutants. The numbers refer to the total number of observed clones.

clone, consisting of one single labeled cell, was recovered at the back of the air sac primordium (Figure 4B). However, we did observe a migration defect for the *Mhc*^{3} allele, on the basis of the finding that only 24% of MARCM mutant *Mhc*^{3} clones reached the distal air sac tip (Figure 4, C and D). These results suggest that *Mhc* is indeed required for tracheal cell migration in the air sac primordium.

These observations also suggest that the cell migration process we analyze is more strongly affected by the *Mhc*^{1} allele than by the *2L2881* allele. *Mhc*^{1} is an embryonic lethal allele: late embryos are devoid of muscles and are incapable of moving and hatching (Mogami *et al.* 1986). In contrast, we did recover viable homozygous *2L2881* first instar larvae (data not shown). Furthermore, staining of F-actin in muscles using TRITC-phalloïdin showed that muscle fibers can still be observed in homozygous *2L2881* embryos, whereas they are absent in *Mhc*^{1} homozygotes (data not shown). Altogether, these results suggest that *2L2881* is a hypomorphic *Mhc* allele.

Mutant lines 2L2896 and 2L3297: 2L2896 and *2L3297* showed a migration phenotype of equivalent strength: in *2L2896*, only 17.2% of MARCM clones were found at the distal tip of the air sac primordium and in *2L3297*, 16% of the clones reached the tip (Table 2 and Figure 5, A, B, and E).

2L2896 and *2L3297* did not complement each other's associated lethality, and both mutations mapped to the overlapping region of *Df(2L)Exel8026* and *Df(2L)Exel7049* (Table 2). This region contains three genes: *DNZDHHC/NEW1 zinc finger protein 11* (*Dnz1*), *IplI-aurora-like kinase* (*ial*), and *signal transducing adaptor molecule* (s*tam*). Since no lethal mutations affecting any of these genes were available, we chose to identify the mutated gene by a systematic sequencing approach. We sequenced the open reading frames of *Dnz1* (828 bp), *ial* (987 bp), and s*tam* (2067 bp) in genomic DNA preparations from *FRT40A* wild-type embryos as well as from homozygous *2L2896* and *2L3297* mutant embryos (see materials and methods).

We did not find any nucleotide change in the *Dnz1* and the *ial* coding region, suggesting that theses genes are not responsible for the lethality in these two mutant lines. However, nucleotide changes were found when comparing the s*tam* gene sequence between the parental, nonmutagenized *FRT40A* chromosome, used as a wild-type control, and both mutant alleles. In *2L2896*, we found a C^{16}-to-T transition and a G^{1513}-to-A transition. The first substitution causes a nonsense mutation from Gln^{6} to a stop codon, and the second mutation induces a transition of an Ala^{505} to a Thr. The presence of a stop codon at amino acid position 6 suggests that *2L2896* does not produce a functional Stam protein and represents a null allele. In the case of *2L3297*, we also detected two nucleotide substitutions: a T^{1283} to C, and a T^{1583} to C. These modifications induce a Phe^{428}-to-Ser and a Tyr^{528}-to-His transition, respectively. It is worth mentioning that an *in silico* analysis revealed that Tyr^{528} is in an environment favorable to tyrosine phosphorylation (data not shown). If Tyr^{528} were indeed

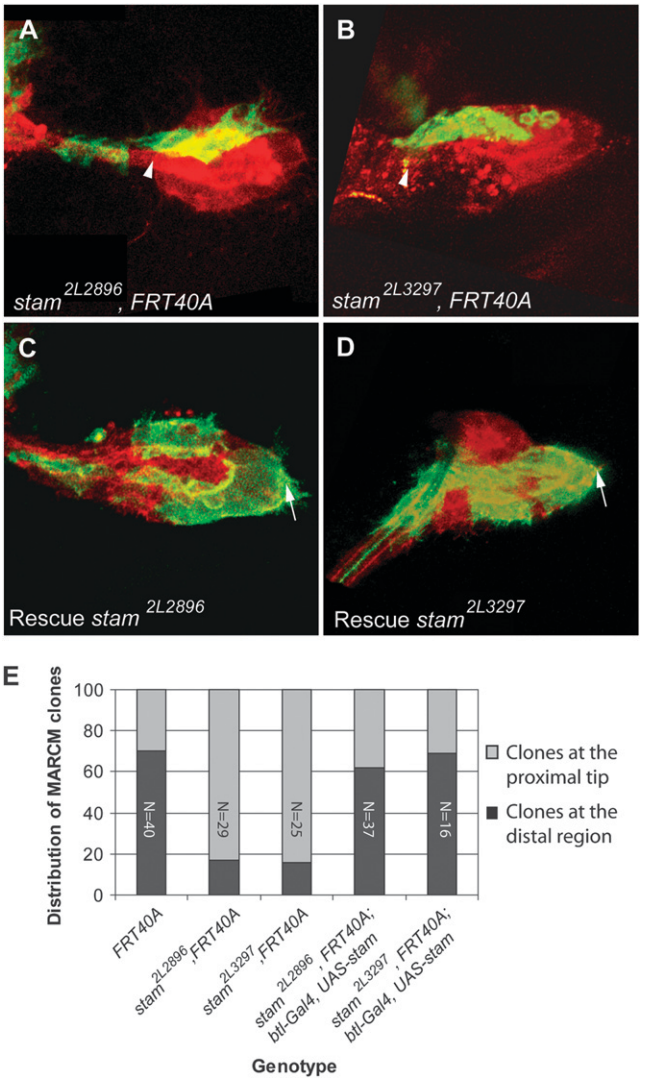

Figure 5.—Homozygous *stam* mutant MARCM clones display a migration phenotype. (A–D) Confocal micrographs of a Drosophila third instar larval dorsal air sac primordium. All tracheal cells are labeled in red (RFP-moesin). Cells belonging to the MARCM clones are labeled in green (CD8-GFP). MARCM clones were induced for the *stam*^{2L2896}, *FRT40A* (A) and for the *stam*^{2L3297}, *FRT40A* (B) mutant. Overexpression of a wild-type *stam* cDNA in tracheal cells of *stam*^{2L2896}, *FRT40A* (C) and *stam*^{2L3297}, *FRT40A* (D) mutants rescued the migration phenotype. Arrows indicate the distal tip of the air sac primordium. Arrowheads indicate the proximal region of the air sac primordium. (E) Graphical representation of the statistical distribution of MARCM clones in the dorsal air sac primordium (gray, localization at the proximal region; black, localization at the distal growing tip). The *FRT40A* chromosome was used as a wild-type control. Wild-type clones colonized the distal tip of the growing air sac primordium in 70% of the cases. This proportion is dramatically reduced in the *stam*^{2L2896}, *FRT40A* and *stam*^{2L3297}, *FRT40A* mutants. Overexpression of *stam* in mutant MARCM clones restored a wild-type migration profile. The numbers refer to the total number of observed clones.

phosphorylated *in vivo*, this post-translational modification would no longer be possible in the *stam*^{2L3297} mutant allele. Further biochemical analyses of the Stam protein are required to test this hypothesis.

To investigate whether the cell migration defects observed in *2L2896* and *2L3297* were indeed due to the mutations we identified in the s*tam* coding region, we overexpressed a *UAS-stam* transgene in homozygous mutant MARCM clones using a *btl-Gal4* driver and observed a full rescue of the migration defects (Figure 5, C and D): 62 and 69% of the rescued MARCM clones reached the distal tip of the air sac primordium in *2L2896* and *2L3297* animals, respectively (Figure 5E). Altogether, these results strongly suggest that the tracheal cell migration phenotypes observed in the *2L2896* and *2L3297* alleles are due to the disruption of s*tam*.

DISCUSSION

A MARCM clones screen for tracheal cell migration defects: To better understand the molecular basis of the important role of FGF signaling in the regulation of cell migration, we conducted an EMS-genetic screen of the left arm of the second chromosome and analyzed the migration of mutant mitotic MARCM clones generated in the dorsal air sac primordium.

Since the analysis of MARCM clones in the air sac requires a labor-intensive dissection step, we restricted our initial screen to 1123 EMS mutant lines. The number of genes present on chromosomal arm 2L is estimated to be between 2700 and 2800. Therefore, the screen we performed was far away from being saturating. Indeed, most of the lethal complementation groups we isolated are represented by a single allele; two individual alleles were recovered only for two complementation groups. In addition, we did not isolate novel alleles of *pten*, which is the only locus located on chromosomal arm 2L known to be required for tracheal cell migration in the air sac primordium (Cabernard and Affolter 2005). However, as this screen indeed allowed us to recover mutations affecting tracheal cell migration, a larger screen on 2L and similar approaches involving the other chromosomal arms should be performed to identify additional factors involved in FGF-dependent tracheal cell migration.

Screen result summary and isolated mutants: Of the 1123 lines we have tested, 122 (11%) displayed no MARCM clones in the tracheal system (Table 1). The corresponding mutations may affect genes implicated in cell viability. Alternatively, the FRT site could be mutated, making recombination no longer possible. Interestingly, in the case of 90 lines (8%), no clones were observed in the air sac primordium although MARCM clones were detected in the mature larval tracheal system (Table 1). During third instar larval development, the second thoracic tracheal metamere is repopulated by tracheoblasts; a small subset of the latter subsequently gives rise to the dorsal air sac primordium (Guha and Kornberg 2005). We postulate that genes required for the process of tracheoblast repopulation would fall into this phenotypic category if mutated.

Forty-seven lines (4%) exhibited a phenotype corresponding to our screening criteria, *i.e.*, <40% of MARCM clones reaching the air sac primordium distal tip. We isolated 34 class I lines bearing a strict migration defect (Table 1). Two of these lines, *2L3267* and *2L2870*, displayed a strict FGFR-like phenotype, as all MARCM clones were observed at the proximal air sac region (Table 2 and Figure 3D). This strong phenotype has so far been observed exclusively for mutants affecting components of the FGFR pathway: *btl/FGFR*, *dof*, *slf*, and *pnt* (Cabernard and Affolter 2005). The *2L3267* and *2L2870* lines do not map to any of these loci and therefore most likely carry mutations affecting essential and novel genes specifically linked to FGF-dependant cell migration. Identification and characterization of these two interesting loci are currently under investigation.

Of the selected candidate lines, nine belong to the class II, since they showed both a tracheal cell migration and a proliferation phenotype. Interestingly, this behavior resembles the phenotype observed for mutations in genes implicated in the Ras/MAPK pathway (Cabernard and Affolter 2005). Therefore, class II mutants could affect factors of this pathway, although it is obviously possible that some EMS-mutated genes identified in the screen code for components unrelated to the regulation of Ras or of its downstream targets. Identification and characterization of these loci will provide more insight into their precise function in the regulation of tracheal cell migration and proliferation.

Mapping strategy of the mutant loci: Using the Exelixis deficiency kit we mapped lethal hits to specific genomic areas on chromosomal arm 2L in 20 candidate lines. For the remaining candidate lines, which are not mapped, we are currently testing the alternative Bloomington 2L deficiency kit, which covers 94.8% of the 2L chromosomal arm. However, we cannot exclude that in some lines the hit responsible for lethality is located on chromosomal arm 2R and is different from the mutation responsible for the migration phenotype located on chromosomal arm 2L.

Identification of the Mhc gene: We identified a lethal hit in the *Mhc* gene. *Mhc* encodes a Myosin heavy chain protein and belongs to the Myosin II class of molecules also termed conventional myosins (Yamashita *et al.* 2000). Although Mhc is known as the muscle Mhc isoform, its function is not restricted to muscles. Indeed, expression of the *Mhc* gene has been shown to be regulated in border cells by the transcriptional regulator Slow border cells (Slbo) (Borghese *et al.* 2006; Wang *et al.* 2006), a key regulator of border cell migration in the egg chamber during oogenesis. Moreover,

border cell migration is impaired in the *Mhc*^{3} allele (Borghese *et al.* 2006). Several genes required for border cell migration, like *slbo*, *pvr* (necessary for Drosophila VEGF-dependent signaling), and *blistered/DSRF*, were previously tested for their possible involvement in tracheal cell migration in the air sac. However, MARCM clones homozygous for mutations in these genes displayed a wild-type migration behavior (C. Cabernard, unpublished results). These results suggest different mechanisms of cell migration depending on cell and tissue context. However, *Mhc* is required in both cases, suggesting that it constitutes a more general actor in cell migration.

Identification of the *stam* gene: In our screen, we identified *2L2896* and *2L3297* as carriers of independent and distinct alleles of the s*tam* locus. Two human Stam homologs have been described (Takeshita *et al.* 1996; Endo *et al.* 2000; Pandey *et al.* 2000; Takata *et al.* 2000). Stam proteins are constitutive binding partners of the Hepatocyte growth factor-regulated substrate (Hrs) (Asao *et al.* 1997; Takata *et al.* 2000). Vertebrate Stam and Hrs colocalize at the level of early endosomes and are involved in vesicle trafficking and sorting of ubiquitinated membrane proteins into multivesicular bodies (MVB) (Bache *et al.* 2003; Kanazawa *et al.* 2003). In mammals, both proteins are known to be involved in the regulation of receptor tyrosine kinase (RTK) signaling via stimulation of the degradation of activated EGFR (for review, see Clague and Urbe 2006 and references therein). In Drosophila, Hrs is also required for MVB maturation and downregulation of several signaling receptors, including RTKs (Lloyd *et al.* 2002; Jekely and Rorth 2003). However, no s*tam* loss-of-function mutants have been described so far in Drosophila, and its function has not been investigated yet. It will be of interest to test whether Drosophila s*tam* regulates tracheal cell migration by regulating protein levels of activated Btl/FGFR. A study investigating this hypothesis will be presented elsewhere.

We thank K. Basler, M. Yoshihara, P. Rorth, the Blomington Stock Center, and the Drosophila Genetic Resource Center (KIT Tokyo) for sending flies; C. Dossenbach for participating in initial steps of the screen; and B. Bruno, G. Evora, and K. Mauro for technical support. We are grateful to B. Bello for invaluable comments on the manuscript. Studies in the laboratory of M. A. are supported by research grants from the Swiss National Science Foundation, the cantons Basel-Stadt and Basel-Land, and the European Commission via the FP6 Network of Excellence "Cells into organs." Studies in the laboratory of M. L. are supported by the International Graduate School in Genetics and Functional Genomics and the Deutsche Forschungsgemeinschaft (grants LE546/3-1 and LE546/3-2).

LITERATURE CITED

Affolter, M., and C. J. Weijer, 2005 Signaling to cytoskeletal dynamics during chemotaxis. Dev. Cell **9:** 19–34.

Affolter, M., S. Bellusci, N. Itoh, B. Shilo, J. P. Thiery *et al.*, 2003 Tube or not tube: remodeling epithelial tissues by branching morphogenesis. Dev. Cell **4:** 11–18.

Asao, H., Y. Sasaki, T. Arita, N. Tanaka, K. Endo *et al.*, 1997 Hrs is associated with STAM, a signal-transducing adaptor molecule. Its suppressive effect on cytokine-induced cell growth. J. Biol. Chem. **272:** 32785–32791.

Bache, K. G., C. Raiborg, A. Mehlum and H. Stenmark, 2003 STAM and Hrs are subunits of a multivalent ubiquitin-binding complex on early endosomes. J. Biol. Chem. **278:** 12513–12521.

Baer, M. M., A. Bilstein and M. Leptin, 2007 A clonal genetic screen for mutants causing defects in larval tracheal morphogenesis in Drosophila. Genetics **176:** 2279–2291.

Borghese, L., G. Fletcher, J. Mathieu, A. Atzberger, W. C. Eades *et al.*, 2006 Systematic analysis of the transcriptional switch inducing migration of border cells. Dev. Cell **10:** 497–508.

Brunner, D., K. Ducker, N. Oellers, E. Hafen, H. Scholz *et al.*, 1994 The ETS domain protein pointed-P2 is a target of MAP kinase in the sevenless signal transduction pathway. Nature **370:** 386–389.

Cabernard, C., and M. Affolter, 2005 Distinct roles for two receptor tyrosine kinases in epithelial branching morphogenesis in Drosophila. Dev. Cell **9:** 831–842.

Cabernard, C., M. Neumann and M. Affolter, 2004 Cellular and molecular mechanisms involved in branching morphogenesis of the Drosophila tracheal system. J. Appl. Physiol. **97:** 2347–2353.

Clague, M. J., and S. Urbe, 2006 Endocytosis: the DUB version. Trends Cell Biol. **16:** 551–559.

Endo, K., T. Takeshita, H. Kasai, Y. Sasaki, N. Tanaka *et al.*, 2000 STAM2, a new member of the STAM family, binding to the Janus kinases. FEBS Lett. **477:** 55–61.

Ghabrial, A., S. Luschnig, M. M. Metzstein and M. A. Krasnow, 2003 Branching morphogenesis of the Drosophila tracheal system. Annu. Rev. Cell Dev. Biol. **19:** 623–647.

Guha, A., and T. B. Kornberg, 2005 Tracheal branch repopulation precedes induction of the Drosophila dorsal air sac primordium. Dev. Biol. **287:** 192–200.

Hogan, B. L., and P. A. Kolodziej, 2002 Organogenesis: molecular mechanisms of tubulogenesis. Nat. Rev. Genet. **3:** 513–523.

Imam, F., D. Sutherland, W. Huang and M. A. Krasnow, 1999 stumps, a Drosophila gene required for fibroblast growth factor (FGF)-directed migrations of tracheal and mesodermal cells. Genetics **152:** 307–318.

Jekely, G., and P. Rorth, 2003 Hrs mediates downregulation of multiple signalling receptors in Drosophila. EMBO Rep. **4:** 1163–1168.

Kanazawa, C., E. Morita, M. Yamada, N. Ishii, S. Miura *et al.*, 2003 Effects of deficiencies of STAMs and Hrs, mammalian class E Vps proteins, on receptor downregulation. Biochem. Biophys. Res. Commun. **309:** 848–856.

Klambt, C., L. Glazer and B. Z. Shilo, 1992 breathless, a Drosophila FGF receptor homolog, is essential for migration of tracheal and specific midline glial cells. Genes Dev. **6:** 1668–1678.

Lee, T., and L. Luo, 1999 Mosaic analysis with a repressible cell marker for studies of gene function in neuronal morphogenesis. Neuron **22:** 451–461.

Lee, T., and L. Luo, 2001 Mosaic analysis with a repressible cell marker (MARCM) for Drosophila neural development. Trends Neurosci. **24:** 251–254.

Lin, X., E. M. Buff, N. Perrimon and A. M. Michelson, 1999 Heparan sulfate proteoglycans are essential for FGF receptor signaling during Drosophila embryonic development. Development **126:** 3715–3723.

Lloyd, T. E., R. Atkinson, M. N. Wu, Y. Zhou, G. Pennetta *et al.*, 2002 Hrs regulates endosome membrane invagination and tyrosine kinase receptor signaling in Drosophila. Cell **108:** 261–269.

Lubarsky, B., and M. A. Krasnow, 2003 Tube morphogenesis: making and shaping biological tubes. Cell **112:** 19–28.

Manning, G., and M. Krasnow, 1993 Development of the Drosophila tracheal system, pp. 609–685 in *The Development of Drosophila*, edited by A. Martinez-Arias and M. Bate. Cold Spring Harbor Laboratory Press, Cold Spring Harbor, NY.

Michelson, A. M., S. Gisselbrecht, E. Buff and J. B. Skeath, 1998 Heartbroken is a specific downstream mediator of FGF receptor signalling in Drosophila. Development **125:** 4379–4389.

Mogami, K., P. T. O'Donnell, S. I. Bernstein, T. R. Wright and C. P. Emerson, Jr., 1986 Mutations of the Drosophila myosin heavy-chain gene: effects on transcription, myosin accumulation, and muscle function. Proc. Natl. Acad. Sci. USA **83:** 1393–1397.

O'Neill, E. M., I. Rebay, R. Tjian and G. M. Rubin, 1994 The activities of two Ets-related transcription factors required for Drosophila eye development are modulated by the Ras/MAPK pathway. Cell **78:** 137–147.

Pandey, A., M. M. Fernandez, H. Steen, B. Blagoev, M. M. Nielsen *et al.*, 2000 Identification of a novel immunoreceptor tyrosine-based activation motif-containing molecule, STAM2, by mass spectrometry and its involvement in growth factor and cytokine receptor signaling pathways. J. Biol. Chem. **275:** 38633–38639.

Parks, A. L., K. R. Cook, M. Belvin, N. A. Dompe, R. Fawcett *et al.*, 2004 Systematic generation of high-resolution deletion coverage of the Drosophila melanogaster genome. Nat. Genet. **36:** 288–292.

Pellegrini, L., 2001 Role of heparan sulfate in fibroblast growth factor signalling: a structural view. Curr. Opin. Struct. Biol. **11:** 629–634.

Reichman-Fried, M., B. Dickson, E. Hafen and B. Z. Shilo, 1994 Elucidation of the role of breathless, a Drosophila FGF receptor homolog, in tracheal cell migration. Genes Dev. **8:** 428–439.

Sato, M., and T. B. Kornberg, 2002 FGF is an essential mitogen and chemoattractant for the air sacs of the drosophila tracheal system. Dev. Cell **3:** 195–207.

Sutherland, D., C. Samakovlis and M. A. Krasnow, 1996 branchless encodes a Drosophila FGF homolog that controls tracheal cell migration and the pattern of branching. Cell **87:** 1091–1101.

Takata, H., M. Kato, K. Denda and N. Kitamura, 2000 A hrs binding protein having a Src homology 3 domain is involved in intracellular degradation of growth factors and their receptors. Genes Cells **5:** 57–69.

Takeshita, T., T. Arita, H. Asao, N. Tanaka, M. Higuchi *et al.*, 1996 Cloning of a novel signal-transducing adaptor molecule containing an SH3 domain and ITAM. Biochem. Biophys. Res. Commun. **225:** 1035–1039.

Thibault, S. T., M. A. Singer, W. Y. Miyazaki, B. Milash, N. A. Dompe *et al.*, 2004 A complementary transposon tool kit for Drosophila melanogaster using P and piggyBac. Nat. Genet. **36:** 283–287.

Uv, A., R. Cantera and C. Samakovlis, 2003 Drosophila tracheal morphogenesis: intricate cellular solutions to basic plumbing problems. Trends Cell Biol. **13:** 301–309.

Vincent, S., R. Wilson, C. Coelho, M. Affolter and M. Leptin, 1998 The Drosophila protein Dof is specifically required for FGF signaling. Mol. Cell **2:** 515–525.

Wang, X., J. Bo, T. Bridges, K. D. Dugan, T. C. Pan *et al.*, 2006 Analysis of cell migration using whole-genome expression profiling of migratory cells in the Drosophila ovary. Dev. Cell **10:** 483–495.

Warburton, D., M. Schwarz, D. Tefft, G. Flores-Delgado, K. D. Anderson *et al.*, 2000 The molecular basis of lung morphogenesis. Mech. Dev. **92:** 55–81.

Whitten, J., 1980 The tracheal system, pp. 499–540 in *The Genetics and Biology of Drosophila*, edited by M. Ashburner and T. R. F. Wright. Academic Press, New York.

Yamashita, R. A., J. R. Sellers and J. B. Anderson, 2000 Identification and analysis of the myosin superfamily in Drosophila: a database approach. J. Muscle Res. Cell Motil. **21:** 491–505.

Communicating editor: K. V. Anderson